

- [9] P. A. Bokhan, "Experiment on optical pumping of a carbon dioxide molecular laser," *Opt. Spectrosc.*, vol. 32, pp. 435-436, 1972.
- [10] O. R. Wood and T. Y. Chang, "Transverse-discharge hydrogen halide lasers," *Appl. Phys. Lett.*, vol. 20, pp. 77-79, 1972.
- [11] T. Y. Chang and O. R. Wood, "A simple self-mode-locked atmospheric pressure CO<sub>2</sub> laser," *IEEE J. Quantum Electron.*, vol. QE-8, pp. 721-723, Aug. 1972.
- [12] J. C. Stephenson, R. E. Wood, and C. B. Moore, "Near resonant energy transfer between infrared active vibrations," *J. Chem. Phys.*, vol. 48, pp. 4780-4791, 1968.
- [13] I. Burak, Y. Noter, and A. Szöke, "Vibration-vibration energy transfer in the  $\nu_3$  mode of CO<sub>2</sub>," *IEEE J. Quantum Electron.*, vol. QE-9, pp. 541-544, May 1973.
- [14] R. L. Taylor and S. Bitterman, "Survey of vibrational relaxation data for processes important in the CO<sub>2</sub>-N<sub>2</sub> laser system," *Rev. Mod. Phys.*, vol. 41, pp. 26-47, 1969.
- [15] B. I. Stepanov, S. A. Trushin, and V. V. Churakov, "Two component molecular laser pumped optically in the 4.3  $\mu$  Band," *Sov. J. Quantum Electron.*, vol. 6, pp. 715-718, 1976.
- [16] (a) A. L. Golger and V. S. Letokhov, "Population inversion of vibrational levels in a high-pressure molecular gas pumped by laser radiation," *Sov. J. Quantum Electron.*, vol. 3, pp. 428-432, 1974.  
 (b) A. L. Golger and V. S. Letokhov, "Amplification in a mixture of isotopic CO<sub>2</sub> molecules pumped by CO<sub>2</sub> laser radiation," *Sov. J. Quantum Electron.*, vol. 5, pp. 811-816, 1975.
- [17] A. V. Eletskii, L. Ya. Efremenkov, and B. M. Smirnov, "Optically pumped carbon dioxide laser," *Sov. Phys.-Doklady*, vol. 15, pp. 843-845, 1971.
- [18] K. G. Brown and W. B. Person, "Preliminary interpretation of the infrared intensities of combination and difference bands of N<sub>2</sub>O and CO<sub>2</sub>," *J. Chem. Phys.*, vol. 65, pp. 2367-2370, 1976.
- [19] H. Kildal and T. F. Deutsch, "Optically pumped infrared v-v transfer lasers," *Appl. Phys. Lett.*, vol. 27, pp. 500-502, 1975.
- [20] T. F. Deutsch and H. Kildal, "Progress in optically pumped CO transfer lasers," *Opt. Commun.*, vol. 18, pp. 124-125, 1976.
- [21] R. M. Osgood, Jr., "Optically pumped 16  $\mu$ m CO<sub>2</sub> lasers," *Appl. Phys. Lett.*, vol. 28, pp. 342-345, 1976.
- [22] M. C. Lin, "Photoexcitation and photodissociation lasers - part I: Nitric oxide laser emissions resulting from C(2\Pi)  $\rightarrow$  A(2\Sigma<sup>+</sup>) and D(2\Sigma<sup>+</sup>)  $\rightarrow$  A(2\Sigma<sup>+</sup>) transitions," *IEEE J. Quantum Electron.*, vol. QE-10, pp. 516-521, June 1974.
- [23] (a) A. B. Petersen, C. Wittig, and S. R. Leone, "Infrared molecular lasers pumped by electronic-vibrational energy transfer from Br(4<sup>2</sup>P<sub>1/2</sub>): CO<sub>2</sub>, N<sub>2</sub>O, HCN, and C<sub>2</sub>H<sub>2</sub>," *Appl. Phys. Lett.*, vol. 27, pp. 305-307, 1975.  
 (b) —, "Electronic-to-vibrational pumped CO<sub>2</sub> laser operating at 4.3, 10.6 and 14.1  $\mu$ m," *J. Appl. Phys.*, vol. 47, pp. 1051-1054, 1976.  
 (c) —, "Infrared molecular lasers pumped by e-v energy transfer," *Opt. Commun.*, vol. 18, pp. 125-126, 1976.
- [24] R. L. Abrams, "Broadening Coefficients for the P(20) CO<sub>2</sub> laser transition," *Appl. Phys. Lett.*, vol. 25, pp. 609-611, 1974.
- [25] T. Y. Chang, "Accurate frequencies and wavelengths of CO<sub>2</sub> laser lines," *Opt. Commun.*, vol. 2, pp. 77-80, 1970.

## Passive Mode Locking of Lasers with the Optical Kerr Effect Modulator

K. SALA, MARTIN C. RICHARDSON, MEMBER, IEEE, AND N. R. ISENOR

**Abstract**—A detailed analytical investigation is presented of a nonlinear device termed the optical Kerr effect modulator (OKEM) which is used to passively *Q* switch and mode lock high-power lasers. Experimentally, an OKEM employing two standard quarter-wave plates is used to passively mode lock the Nd:glass laser. The mode-locking threshold dependence upon the parameters of the OKEM transmission function is definitively established. Pulsewidths and spectral measurements are given for the train of ultrashort pulses from the glass laser mode locked with the OKEM using two different Kerr liquids. The analytical and experimental results together indicate that the OKEM technique is a versatile and viable alternative and in addition overcomes most of the

shortcomings intrinsic to the saturable absorber technique. The non-resonant nature of the OKEM suggests that it should find immediate application as a passive *Q*-switching and mode-locking element for a variety of lasers, including dye lasers, UV lasers, the CO<sub>2</sub> laser, and, notably, the high-power iodine laser.

### I. INTRODUCTION

WHILE the use of saturable absorbers for passive mode locking is a straightforward and simple technique, numerous investigations of the technique have revealed a number of intrinsic shortcomings, particularly evident with high-power pulsed lasers such as Nd:glass [1], [2]. There exists, however, an alternate passive mode-locking technique based upon the phase modulation characteristics of the optical Kerr effect (OKE) which compares favorably with the simplicity of the saturable absorber method while providing a much greater degree of versatility and control over the mode-locking kinetics. The basic device, hereafter referred to as the optical Kerr effect modulator (OKEM), is illustrated schematically in Fig. 1. The transmission for a round trip through the OKEM is a function of the orientations and retardances of the wave

Manuscript received March 1, 1977; revised July 5, 1977. A paper describing these results was presented at the Joint Congress of the CAP-APS-SMF, Quebec, Canada, June 1976. Work on this paper performed by K. Sala was supported by the National Research Council of Canada Ottawa, Ont., Canada, and was submitted to the Department of Physics, University of Waterloo, Waterloo, Ont., Canada, in partial fulfillment of the requirements for the Ph.D degree.

K. Sala and M. C. Richardson are with the Division of Physics, National Research Council of Canada, Ottawa, Ont., Canada.

N. R. Isenor was with the Division of Physics, National Research Council of Canada, Ottawa, Ont., Canada. He is now with the Department of Physics, University of Waterloo, Waterloo, Ont., Canada.

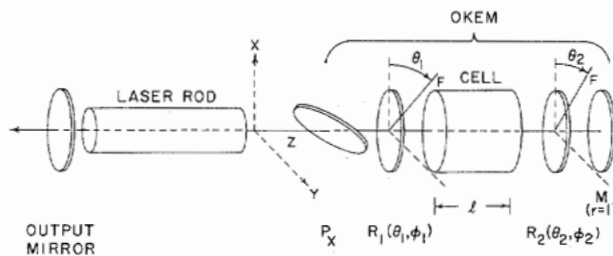


Fig. 1. OKEM.  $R_1, R_2$  = retardation plates;  $M$  = fully reflecting dielectric mirror;  $P_x$  = thin film reflection polarizer.

plates and of the self-induced ellipse rotation (SIER) occurring in the cell. Since the SIER is intensity- and polarization-state dependent, it is possible to select suitable values for the orientation angles and the retardances such that the OKEM transmission as a function of intensity resembles that of a saturable absorber. The first reported use of the OKE for passive mode locking came in 1968 from Comly *et al.* [3] who utilized a cell of heated nitrobenzene or  $\alpha$ -chloronaphthalene in a ruby laser conventionally  $Q$  switched by a rotating mirror. The possible use of SIER for simultaneous  $Q$  switching and mode locking was first raised in a general sense by Glenn [4]. Shortly thereafter, Dahlström independently proposed and successfully used the OKEM to passively  $Q$  switch and mode lock the Nd:glass laser [5]. However, an apparent lack of numerical parameters makes duplication difficult and since 1972 no further reports on this approach have been made.

The present paper presents a detailed analysis of the transmission properties of the OKEM for arbitrary values of the retardances. A closed analytical expression for the OKEM transmission is derived. It is then shown that the value of the first retardance is a redundant parameter in this expression with the result that, with only three independent parameters to consider, the problem is considerably simplified. A specific version of the OKEM which employs two standard quarter-wave retarders is studied analytically. The OKEM  $Q$ -switched and mode-locked Nd:glass laser is investigated experimentally and the mode-locking threshold dependence on key transmission function parameters is established. Pulsewidth and spectral measurements of the mode-locked picosecond pulses are presented. The paper concludes with a brief discussion of further developments and applications of the OKEM mode-locking technique.

## II. THE TRANSMISSION OF THE OKEM

The various elements of the OKEM are described by their Jones matrices [6] presently written to conform with a positive phase convention defined as  $\exp [i(kz - \omega t + \delta)]$ . The fully reflecting mirror adjacent to the retarder  $R_2$  has the Jones matrix

$$D = \begin{pmatrix} 1 & 0 \\ 0 & -1 \end{pmatrix} \quad (1)$$

while the polarizer  $P_x$  is described by

$$P_x = \begin{pmatrix} 1 & 0 \\ 0 & 0 \end{pmatrix}. \quad (2)$$

It is assumed that the only linear loss in the resonator is that due to the output mirror. The retardation plates are described by the product matrices  $R(\theta_j, \phi_j) = e^{i\beta_j} M(-\theta_j) R(\phi_j) M(\theta_j)$ ,  $j = 1, 2$  where

$$M(\theta_j) = \begin{pmatrix} \cos \theta_j & \sin \theta_j \\ -\sin \theta_j & \cos \theta_j \end{pmatrix}, \text{ and } R(\phi_j) = \begin{pmatrix} \exp -i\phi_j/2 & 0 \\ 0 & \exp i\phi_j/2 \end{pmatrix} \quad (3)$$

are the coordinate rotation and retardation matrices, respectively. The dispersion factor is  $\beta_j = (n_s + n_f) (\phi_j + 2N_j\pi) / 2(n_s - n_f)$  where  $n_f$  and  $n_s$  are the fast and slow refractive indices and  $N_j$  is the order of the  $j$ th plate. The orientation angles  $\theta_j$  of the fast axes are measured positively for rotation from the  $+x$ -axis towards the  $+y$ -axis as indicated in Fig. 1.

An origin  $z = 0$  is defined to lie between the laser rod and the polarizer  $P_x$  (Fig. 1). A quasi-monochromatic Gaussian model is adopted to describe the electric field (at  $z = 0$ ) as

$$E_{in}(t) = E_0 \exp [-(t/\tau)^2/2] \cos \omega_0 t; \\ I_{in}(t) = I_0 \exp [-(t/\tau)^2] \quad (4)$$

where the peak time averaged pulse intensity is  $I_0 = cE_0^2/8\pi$  and  $2\tau$  is the full  $e^{-1}$  pulse duration. The subscripts "in" and "out" are understood to refer to the radiation entering and leaving the OKEM, respectively. The SIER within the cell is described by the intensity-dependent rotation matrix [7], [8]  $N(\epsilon_j) = \exp [i\Gamma + i\beta_0] M(\epsilon_j)$ ,  $j = 1, 2$  where the self-phase modulation (SPM) factor is

$$\Gamma = (\delta n_+ + \delta n_-) \omega_0 l / 2c \\ = \frac{48\pi^2 \omega_0 l}{n_0^2 c^2} \chi_3^{1111}(\omega_0, \omega_0, \omega_0, -\omega_0) I_0 \exp -(t/\tau)^2 \quad (5)$$

and the linear dispersion factor is  $\beta_0 = n_0 \omega_0 l / c$  where  $n_0 = n(\omega_0)$ . The SIER angles  $-\epsilon_j = (\delta n_+ - \delta n_-) \omega_0 l / 2c$  for the first transit through the cell from  $R_1$  to  $R_2$  ( $j = 1$ ) and for the return transit from  $R_2$  to  $R_1$  ( $j = 2$ ) can be expressed as [8]  $\epsilon_j = P_j J(t)$  where  $P_j$  is the polarization factor  $P_j = [|E_+|^2 - |E_-|^2]/E_0^2$  and  $J(t)$  is a dimensionless "intensity"  $J(t) = J_0 \exp [-(t/\tau)^2]$  with

$$J_0 = \frac{48\pi^2 \omega_0 l}{n_0^2 c^2} \chi_3^{1221}(\omega_0, \omega_0, \omega_0, -\omega_0) I_0. \quad (6)$$

The circular electric field amplitudes are defined by  $E_{\pm} = 2^{-1/2} (E_x \pm iE_y)$ . The sense of ellipse rotation for SIER may be defined unambiguously as follows: for  $\text{Re}(\chi_3^{1221}) > 0$ , the polarization ellipse will rotate in the same direction in which the electric field vector rotates in time. It is assumed that the nonlinear susceptibility tensor  $\chi_3(\omega_0, \omega_0, \omega_0, -\omega_0)$  is strictly real so that SIER occurs in the absence of any self-induced circular dichroism. Note also that relaxation effects for the self-induced birefringence are assumed negligible (for a pulse duration  $\gtrsim$  the orientational relaxation time of the Kerr liquid, the amount of SIER will be significantly reduced [5]).

The amplitude transmittance for a single round-trip transit through the OKEM is given by the matrix [8]

$$\Upsilon = \begin{pmatrix} \Upsilon_{11} & 0 \\ 0 & 0 \end{pmatrix} = P_x R(-\theta_1, \phi_1) N(\epsilon_2) R(-\theta_2, \phi_2) \\ \cdot DR(\theta_2, \phi_2) N(\epsilon_1) R(\theta_1, \phi_1) P_x \quad (7)$$

while two intermediate amplitude matrices

$$\Upsilon_j = \begin{pmatrix} (\Upsilon_j)_{11} & 0 \\ 0 & 0 \end{pmatrix}; \quad j = 1, 2 \quad (8)$$

are defined as

$$\Upsilon_1 = R(\theta_1, \phi_1) P_x, \text{ and } \Upsilon_2 \\ = R(-\theta_2, \phi_2) DR(\theta_2, \phi_2) N(\epsilon_1) R(\theta_1, \phi_1) P_x. \quad (9)$$

In terms of the matrices  $\Upsilon_j$ , which describe the polarization ellipse entering the cell, the polarization factors are  $P_j = i[(\Upsilon_j)_{11}^* (\Upsilon_j)_{21} - (\Upsilon_j)_{11} (\Upsilon_j)_{21}^*]$ . The electric field emerging from the OKEM is

$$E_{\text{out}}(t) = \text{Re}[\Upsilon_{11} E_0 \exp -(t/\tau)^2/2 \exp -i\omega_0 t]. \quad (10)$$

The amplitude transmittance given by (7) eventually reduces to [8]

$$\Upsilon_{11} = \exp [2i\Gamma + 2i(\beta_0 + \beta_1 + \beta_2)] \{ [\cos \phi_1 \cos \phi_2 \cos \Delta \\ - \sin \phi_1 \sin \phi_2 \cos (\theta + \Sigma)] \\ + i[\sin 2\theta_1 \sin \phi_2 \sin (\theta + \Sigma) \\ - \cos 2\theta_1 \cos \phi_1 \sin \phi_2 \cos (\theta + \Sigma) \\ - \cos 2\theta_1 \sin \phi_1 \cos \phi_2 \cos \Delta]\}. \quad (11)$$

However, for a single transit through the OKEM and for values of  $J_0 < 5$ , the effects of SPM ( $\Gamma$ ) and dispersion ( $\Gamma$  and  $\beta_0, \beta_1, \beta_2$ ) on the output pulse will generally be negligible. Thus the instantaneous intensity transmission of the OKEM,  $T_I = I_{\text{out}}(t)/I_{\text{in}}(t)$ , is simply  $|\Upsilon_{11}|^2$  and takes the form

$$T_I(\theta_1, \theta_2, \phi_1, \phi_2; J) = 1 - \cos^2 \phi_2 \sin^2 \Delta - [A_1 \cos \Delta \\ + A_2 \sin (\theta + \Sigma) + A_3 \cos (\theta + \Sigma)]^2 \quad (12)$$

where  $A_1 = \sin 2\theta_1 \sin \phi_1 \cos \phi_2$ ,  $A_2 = \cos 2\theta_1 \sin \phi_2$ ,  $A_3 = \sin 2\theta_1 \cos \phi_1 \sin \phi_2$ , and where  $\theta = 2\theta_2 - 2\theta_1$ ,  $\Delta = \epsilon_2 - \epsilon_1$ , and  $\Sigma = \epsilon_2 + \epsilon_1$ . The SIER angles are  $\epsilon_1 = P_1 J(t)$  and  $\epsilon_2 = P_2 J(t)$  where  $P_1 = \sin 2\theta_1 \sin \phi_1$ , and  $P_2 = -\sin 2\theta_1 \sin \phi_1 \cos 2\phi_2 - \cos 2\theta_1 \sin (\theta + 2\epsilon_1) \sin 2\phi_2 - \sin 2\theta_1 \cos (\theta + 2\epsilon_1) \cos \phi_1 \sin 2\phi_2$ .

The OKEM transmission is thus described by the analytical expression for  $T_I$  given in (12). However, this formula also reveals that there exists a multitude of possible transmission functions corresponding to the combinations of the four independent parameters  $\theta_1, \theta_2, \phi_1$ , and  $\phi_2$ . Fortunately, a closer examination of the expression for  $T_I(\theta_1, \theta_2, \phi_1, \phi_2; J)$  leads to the discovery that in fact only three of the four parameters are independent with the value of  $\phi_1$  being the redundant parameter. This finding is most clearly expressed by the following theorem [8].

For  $\theta_1, \theta_2, \phi_1$  arbitrary, there exist  $\theta'_1, \theta'_2$  such that

$$T_I(\theta'_1, \theta'_2, \phi_1 = \pi/2, \phi_2; J) = T_I(\theta_1, \theta_2, \phi_1, \phi_2; J).$$

As an immediate consequence of this theorem, the completely general OKEM transmission may thus be rewritten in the reduced form with  $\phi_1 = \pi/2$  as

$$T_I(\theta_1, \theta_2, \phi_2; J) = 1 - \cos^2 \phi_2 \sin^2 \Delta - [A_1 \cos \Delta \\ + A_2 \sin (\theta + \Sigma)]^2 \quad (13)$$

where now  $A_1 = \sin 2\theta_1 \cos \phi_2$ ,  $A_2 = \cos 2\theta_1 \sin \phi_2$ , with  $P_1 = \sin 2\theta_1$  and  $P_2 = -\sin 2\theta_1 \cos 2\phi_2 - \cos 2\theta_1 \sin (\theta + 2\epsilon_1) \sin 2\phi_2$ . Thus, in practice, the most general OKEM can be constructed by using a  $\lambda/4$  plate for  $R_1$  and a variable retardance device for  $R_2$ .

### III. THE OKEM USING TWO QUARTER-WAVE PLATES

When the symmetry of the expression for  $T_I(\theta_1, \theta_2, \phi_2; J)$  in (13) is accounted for, it is found necessary to vary  $\theta_1$  and  $\theta_2$  only over the range of 0 to  $\pi/2$  and  $\phi_2$  over the range of 0 to  $\pi$  in order to calculate all possible transmission functions for the OKEM. Specifically, the complete set of symmetry relations are:

$$\begin{aligned} T_I(\theta_1, \theta_2, \phi_2; J) &= T_I(\theta_1 \pm \pi, \theta_2, \phi_2; J) \\ &= T_I(\theta_1, \theta_2 \pm \pi, \phi_2; J) \\ &= T_I(\theta_1, \theta_2, \phi_2 \pm \pi; J) \\ &= T_I(-\theta_1, -\theta_2, \phi_2; J) \\ &= T_I(\theta_1, \theta_2 + 90^\circ, \pi - \phi_2; J) \\ &= T_I(-\theta_1, -\theta_2 + 90^\circ, \pi - \phi_2; J). \end{aligned} \quad (14)$$

The transmission curves  $T_I = T_I(J_0)$  were computed for  $J_0$  from 0 to 3 in steps of 0.25 while varying the parameters  $\theta_1, \theta_2$ , and  $\phi_2$  independently in  $5^\circ$  increments over those ranges listed above (13 357 curves in all). These transmission curves were then individually examined to determine those  $\phi_2$  values which resulted in saturable absorber-like transmission functions. It was found that such transmission curves occurred only in the range  $\pi/4 < \phi_2 < 3\pi/4$ , with the greatest frequency of occurrence for  $\phi_2$  values between  $80^\circ$  and  $90^\circ$ . In view of this finding and with an eye to keeping the OKEM a practical device employing standard optical components, it was decided to investigate in detail the OKEM using a  $\phi_2$  value of  $\lambda/4$  for the second retarder  $R_2$ .

With  $\phi_2 = \pi/2$ , the OKEM intensity transmission function of (13) for the peak intensity  $J_0$  simplifies to

$$T_I(J_0) = 1 - \cos^2 2\theta_1 \sin^2 (\theta + 2J_0 \sin 2\theta_1). \quad (15)$$

The transmission curves generated by (15) may be accurately characterized by three parameters, namely the initial transmission

$$T_0 \equiv T_I(J_0 = 0) = 1 - \cos^2 2\theta_1 \sin^2 \theta, \quad (16)$$

the initial slope of the transmission function

$$DT_I \equiv \frac{d}{dJ_0} T_I(J_0) \Big|_{J_0=0} = -2 \cos^2 2\theta_1 \sin 2\theta_1 \sin 2\theta, \quad (17)$$

and a value of the intensity  $J_{IP}$  at which  $T_I$  first reaches 100 percent,

$$J_{IP} = \frac{-\theta}{2 \sin 2\theta_1}. \quad (18)$$

Alternatively, in closer analogy to a saturable absorber, one may define a "saturation intensity"  $J_{IS}$  as

$$J_{IS} = \frac{-\theta + \arcsin \left[ \frac{(1 - T_0^{1/2})^{1/2}}{(1 - T_0)^{1/2}} \sin \theta \right]}{2 \sin 2\theta_1} \quad (19)$$

such that  $T_I(J_{IS}) = T_0^{1/2}$  (this corresponds to a reduction in the "absorption coefficient" by a factor of two). In terms of the actual laser intensity, the absolute initial slope of the intensity transmission is

$$\begin{aligned} \frac{d}{dI_0} T(J_0) \Big|_{I_0=0} &= DT_I \frac{dJ_0}{dI_0} \\ &= DT_I \left[ \frac{48\pi^2\omega_0 l}{n_0^2 c^2} \chi_3^{1221}(\omega_0, \omega_0, \omega_0, -\omega_0) \right]. \end{aligned} \quad (20)$$

Fig. 2(a) shows the variation of the parameters  $DT_I$ ,  $J_{IP}$ , and  $J_{IS}$  versus  $\theta_1$  for  $T_0$  a constant and = 50 percent over that range of  $\theta_1$ , where  $DT_I$  is positive. Similar curves are readily calculated for other  $T_0$  values using (16)-(19) and are most useful in practice since they allow a particular transmission function with well-defined characteristics to be chosen without actually having to compute the transmission curve from (15). The maximum value of  $DT_I$  for a given value of  $T_0$  is simply  $2T_0(1 - T_0)^{1/2}$ . Fig. 2(b) shows the dependence of  $DT_I|_{\max}$  and  $DT_I|_{\max}/T_0$  on  $T_0$  and will prove valuable in a discussion to follow where the significance of  $DT_I$  is made clear by the experimental findings. It is noted at this point that, in Fig. 2(a) and in the work to follow, the values of  $\theta_1$  and  $\theta_2$  are taken to lie in the range  $[\pi/2, \pi]$ .

In many respects, a truer measure of the OKEM transmission is the net energy transmission derived by integrating with respect to time the product  $I_{in}(t)T_I(J_0, t)$  and dividing by the net input pulse energy. For the OKEM employing two  $\lambda/4$  plates and  $I_{in}(t)$  given by (4), the net energy transmission is given by

$$T_E(J_0) = (\pi\tau^2)^{-1/2} \int_{-\infty}^{\infty} \exp(-(t/\tau)^2) T_I(J_0, t) dt \quad (21)$$

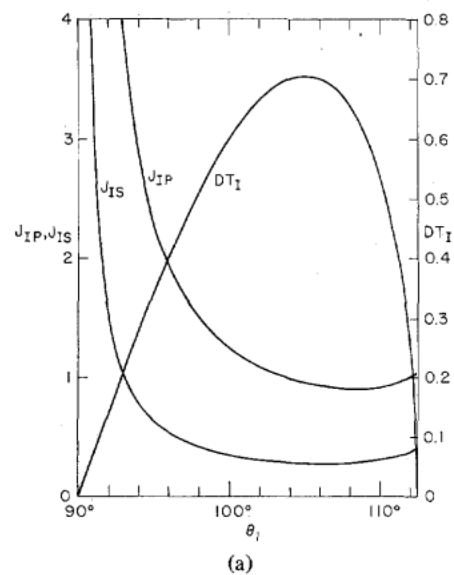
where  $T_I(J_0, t)$  is given by (15) with  $J_0$  replaced by  $J(t)$ . The solution for  $T_E(J_0)$  takes the form

$$\begin{aligned} T_E(J_0) &= (1 - \cos^2 2\theta_1 \sin^2 \theta) \\ &\quad - [\cos^2 2\theta_1 \cos 2\theta] F_1(2J_0 \sin 2\theta_1) \\ &\quad - \frac{1}{2} [\cos^2 2\theta_1 \sin 2\theta] F_2(2J_0 \sin 2\theta_1) \end{aligned} \quad (22)$$

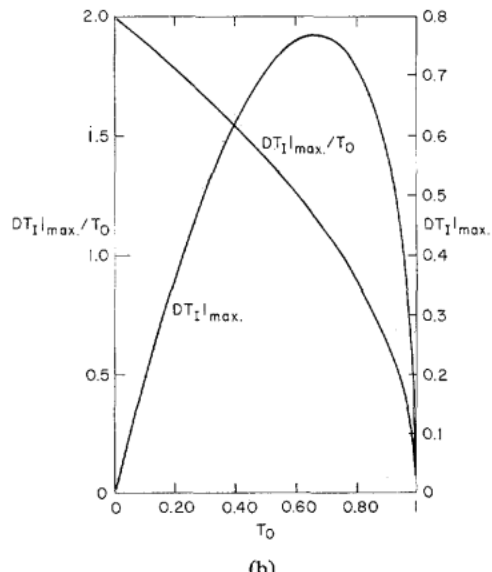
where the functions  $F_1(x)$  and  $F_2(x)$  are given by

$$F_n(x) = \pi^{-1/2} \int_{-\infty}^{\infty} \exp(-y^2) \sin^{3-n}(nx e^{-y^2}) dy; \quad n = 1, 2. \quad (23)$$

The values of  $F_1(x)$  and  $F_2(x)$  must be found numerically. For  $|x| < 5$ , a good approach is to expand the  $\sin^{3-n}$  term in a power series and integrate term by term. For very large



(a)



(b)

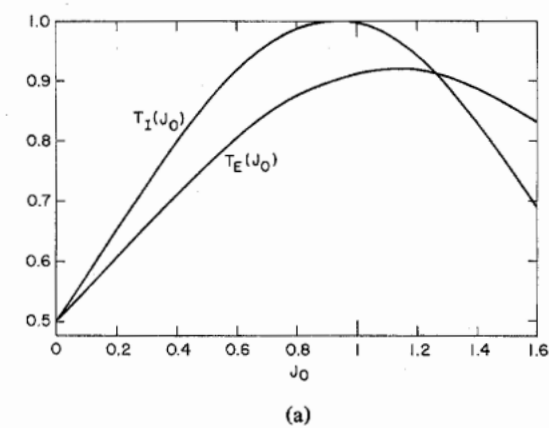
Fig. 2. (a) Variation of  $DT_I$ ,  $J_{IP}$ , and  $J_{IS}$  with  $\theta_1$  for  $T_0 = 0.50$ .  
 (b) Variation of  $DT_I|_{\max}$  and  $DT_I|_{\max}/T_0$  with  $T_0$ .

$|x|$ , the more practical approach for the numerical integration is to use a Hermite-Gaussian quadrature formula. It follows immediately from (21) that  $T_E(J_0 = 0) = T_0$  and  $DT_E \equiv dT_E(J_0 = 0)/dJ_0 = DT_I/2^{1/2}$ . Analogous to the parameters  $J_{IP}$  and  $J_{IS}$  for  $T_I(J_0)$ , expressions for the peak transmission and "saturation" intensities  $J_{EP}$  and  $J_{ES}$  for  $T_E(J_0)$  may be derived [8] in terms of the functions  $F_1$  and  $F_2$  although in practice it is simpler to determine  $J_{EP}$  and  $J_{ES}$  from the calculated  $T_E(J_0)$  transmission curves.

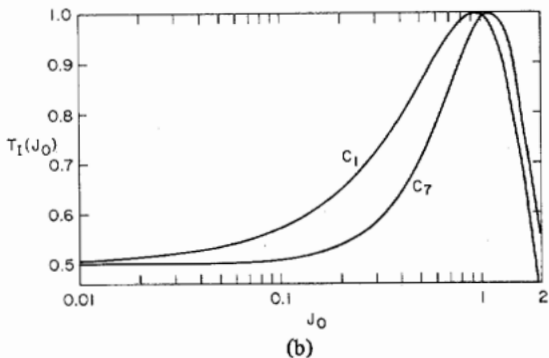
Table I lists the characteristics of 11 transmission curves selected for study experimentally. The curves  $C_1$  to  $C_7$ , all having  $T_0 = 50$  percent, are chosen such that the initial slope parameter  $DT_I$  varies markedly from 0 to 0.7 while, for example, the parameter  $J_{IP}$  remains relatively constant in comparison. The curves  $C_1$  to  $C_7$  will be used to measure experimentally the lasing threshold dependence upon  $DT_I$ . For illustration, Fig. 3(a) plots the transmission functions  $T_I(J_0)$  and  $T_E(J_0)$  for the curve  $C_1$ . The simple  $\sin^2$  behavior for  $T_I(J_0)$  is a characteristic of the OKEM using two

TABLE I  
SELECTED OKEM TRANSMISSION FUNCTIONS  $C_1$  TO  $C_{11}$

	$T_0$	$\theta_1$	$\theta_2$	$\theta$	$DT_I$	$J_{IS}$	$J_{ES}$	$J_{IP}$	$J_{EP}$
$C_1$	0.50	106.10	134.44	56.6818	0.70	0.277	0.394	0.928	1.122
$C_2$	0.50	109.10	141.17	64.1306	0.60	0.291	0.411	0.905	1.090
$C_3$	0.50	110.40	144.94	69.0827	0.50	0.313	0.440	0.923	1.108
$C_4$	0.50	111.30	148.23	73.8664	0.40	0.342	0.478	0.952	1.142
$C_5$	0.50	111.80	150.57	77.5369	0.30	0.369	0.511	0.981	1.171
$C_6$	0.50	112.20	153.08	81.7656	0.20	0.406	0.560	1.020	1.216
$C_7$	0.50	112.50	157.50	90.0000	0.00	0.494	0.675	1.111	1.318
$C_8$	0.90	114.40	128.75	28.6910	0.55	0.100	0.144	0.333	0.406
$C_9$	0.75	112.80	135.61	45.6128	0.70	0.172	0.248	0.557	0.676
$C_{10}$	0.25	102.30	138.43	72.2650	0.40	0.445	0.618	1.515	1.817
$C_{11}$	0.10	97.40	136.84	78.8836	0.18	0.686	0.940	2.695	3.220



(a)



(b)

Fig. 3. (a) OKEM transmission function  $C_1$ . (b) OKEM transmission functions  $C_1$  and  $C_7$  versus  $\log(J_0)$ .

$\lambda/4$  plates; the net transmission  $T_E(J_0)$ , however, tends to be a much smoother function of the intensity. Fig. 3(b) illustrates the significance of the parameter  $DT_I$  for small  $J_0$  values by plotting the transmission function  $T_I(J_0)$  for the two curves  $C_1$  and  $C_7$  versus  $\log(J_0)$ .

At this point it is worthwhile to establish the absolute relationship between the parameter  $J_0$  and the laser intensity

$I_0$  for some OKE media. The experimentally determined results of Owyoung [9] and Wang [10] when extrapolated [11]–[13] to  $\lambda_0 = 1.06 \mu$  give the values  $\chi_3^{1221} \simeq 34 \times 10^{-14}$  ESU in  $CS_2$  and  $\chi_3^{1221} \simeq 20 \times 10^{-14}$  ESU in  $C_6H_5NO_2$ . The electronic portion of  $\chi_3^{1221}$  is given by [8]  $(1 + 12n_2^0/7n_2^e)^{-1}$  where  $n_2^0$  and  $n_2^e$  are, respectively, the orientational and electronic parts of the total nonlinear refractive index  $n_2 = n_2^0 + n_2^e$ ; in  $CS_2$ , the electronic portion of  $\chi_3^{1221}$  is [9]  $\simeq 8$  percent while in nitrobenzene this fraction is [13], [14]  $\simeq 15$  percent. With the above values for  $\chi_3^{1221}$ , (6) yields the results

$$J_0 \simeq \frac{I_0}{800 \text{ MW/cm}} \text{ in } CS_2, \text{ and}$$

$$J_0 \simeq \frac{I_0}{1200 \text{ MW/cm}} \text{ in } C_6H_5NO_2. \quad (24)$$

For comparison, the transmission of a saturable absorber may be described by the transcendental equation [15]

$$\ln [T_0/T(I_0)] + (I_0/I_{\text{sat}}) [1 - T(I_0)] = 0 \quad (25)$$

where, for example, the saturation intensity  $I_{\text{sat}}$  for both the Kodak dyes 9740 and 9860 is [16]  $\simeq 50 \text{ MW/cm}^2$ . From (25),

$$\left. \frac{d}{dI_0} T(I_0) \right|_{I_0=0} = \frac{T_0(1 - T_0)}{I_{\text{sat}}} \quad (26)$$

for a saturable dye, thus revealing that, for a given initial transmission  $T_0$ , the initial slope parameter is a constant along with  $I_{\text{sat}}$ . This is in marked contrast to the case for the OKEM whose transmission is described in (15)–(20). This inflexibility of the saturable absorber's transmission characteristics forbids any modeling of the transmission function which governs the  $Q$ -switching and mode-locking process.

It is apparent that the output pulse emerging from the OKEM,  $I_{\text{out}}(t) = T_I(J_0, t)I_{\text{in}}(t)$ , will have a different temporal

profile than that of the input pulse. For saturable-absorber-like transmission functions such as those for curves  $C_1$  to  $C_{11}$  in Table I, the output pulse will be compressed in time in comparison to  $I_{in}(t)$  when  $J_0 < J_{IP}$ . In the region  $J_{IP} < J_0 < J_{EP}$ , the wings of the pulse will experience a proportionally greater transmission than the peak of the pulse although the net change is still one of compression. If  $J_0 > J_{EP}$ , however, the overall output pulselwidth will exceed that of the input pulse and, in the limit of  $J_0 \gg J_{EP}$ , the output pulse would be expected to have pronounced substructure (it appears unlikely, however, that such large values of  $J_0$  can be realized in view of the dependence of  $T_E(J_0)$  on intensity).

The remarks just given concerning pulse compression as well as the transmission equations given in this paper apply only to the "passive" OKEM in that they characterize the transmission for a single transit through the OKEM of an input pulse having a perfectly smooth Gaussian profile. The transmission functions derived under these assumptions are essentially exact. Numerous studies of SPM and self-steepening [17] have shown that typically the pulse distortion produced by these mechanisms (coupled with linear dispersion) is appreciable only for values  $J_0 \gtrsim 5$ . As well, for a pulse with a reasonably smooth spatial profile, it is always possible to obtain appreciable SIER in a distance much less than the self-focusing length [4]. Furthermore, the self-focusing threshold is higher for elliptically polarized light than for linearly polarized radiation of the same intensity [10], [18]. Hence, since the maximum value of  $J_0$  one may expect to encounter for the OKEM transmissions such as  $C_1$  to  $C_{11}$  is  $J_0 \lesssim 4$ , the effects of SPM, self-steepening, and self-focusing should be negligible for a single transit of a temporally and spatially smooth optical pulse. However, when the OKEM is used as an integral part within the laser resonator, it is necessary to consider the effects of these various nonlinear phenomena over a large number of consecutive transits of the evolving laser pulse within the resonator. In many respects, the distorting effects of a process such as SPM are accumulative, leading to a gradual degradation of the laser pulse [19]. For this reason, the only meaningful way to more exactly determine the OKEM characteristics for very high intensities is to consider this problem as but a part of the more general study of the pulse evolution in a laser passively mode locked with the OKEM.

#### IV. EXPERIMENTAL STUDIES OF THE OKEM MODE-LOCKED ND:GLASS LASER

##### A. The Laser Construction

A parametric study was undertaken of the performance of an OKEM mode-locked Nd:glass laser of the form shown schematically in Fig. 1. The laser resonator was formed by a fully reflecting 5-m radius of curvature dielectric mirror separated 1.2 m from a flat output mirror having a reflectivity of either 0.5, 0.7, or 0.95. A  $9 \times \frac{5}{8}$ -in Brewster-angled laser rod was employed and an iris, situated between the laser rod and polarizer, was used to limit transverse mode structure. The polarizer  $P_x$  was a thin film multilayer dielectric polarizer with principal transmittances of 0.99 and  $4 \times 10^{-3}$  for a single pass. The retardation plates were zero-order, quartz

$\lambda/4$  plates suitably mounted to permit rotation to any desired orientation with an accuracy of  $0.1^\circ$ . The fast and slow axes of the retarders were determined absolutely by calibrating each against a Fresnel rhomb. The cell containing the Kerr liquid was a cylindrical piece of Teflon with an inner diameter of 1 in and fitted with a threaded nylon stop and  $O$  ring. A number of such cells were used which varied in length from 1 to 12 cm. The retarder faces, the second surface of  $P_x$ , and the outside faces of the Kerr cell windows were antireflection coated ( $r < 0.2$  percent per surface). The laser rod and polarizer  $P_x$  were orientated such that the transmitting axis of the OKEM corresponded to horizontal polarization. In practice, either the horizontally polarized beam from the laser output mirror or the predominantly vertically polarized "rejected" beam from  $P_x$  could serve as the laser output, the latter being preferred when the reflectivity of the output mirror was high and/or a very low  $T_0$  value was used for the OKEM.

##### B. Threshold Dependence for Mode Locking with the OKEM

The ability of the OKEM to passively  $Q$  switch and mode lock the Nd:glass laser was investigated for a variety of very different OKEM transmission functions and most systematically for the curves  $C_1$  to  $C_{11}$  of Table I. The Kerr liquids used were carbon disulphide and nitrobenzene at room temperature. For those transmission curves for which mode locking was obtained, a characteristic invariably observed was the existence of two distinct lasing thresholds [20]. A first lower threshold corresponded to the laser operating in the free-running mode. This output was similar [8] to that observed from a normal free-running laser with the exception that the individual spikes in the output showed a pronounced modulation, due to the presence of the Kerr liquid within the laser resonator. As the pumping level was increased, a second threshold was realized at which  $Q$  switching and mode locking of the laser occurred. Fig. 4 shows a typical  $Q$ -switched envelope and the train of ultrashort pulses obtained from the Nd:glass oscillator passively mode locked with the OKEM using  $CS_2$ . The ultrashort pulse trains obtained from the glass laser mode locked with the OKEM using  $C_6H_5NO_2$  were essentially identical to that shown in Fig. 4 although generally more energetic. The transition from the free-running to the mode-locked regime was unmistakable and dramatic, and generally represented a sudden increase in the peak output power by a factor of  $\gtrsim 10^5$ .

While for certain transmission functions it was found that the mode-locking threshold was only very slightly higher than the free-running threshold, it was also observed that for certain other transmission curves this second threshold was very much larger than the free-running threshold. Furthermore, for some of the transmission functions employed, no  $Q$  switching and mode locking were observed despite extremely high pumping levels. As more varied transmission curves were studied, it became apparent that the ease with which mode locking was obtainable depended critically upon the absolute initial slope parameter given in (20). To study this dependence systematically, the two lasing thresholds were measured for the transmission curves  $C_1$  to  $C_7$  of Table I while keeping all

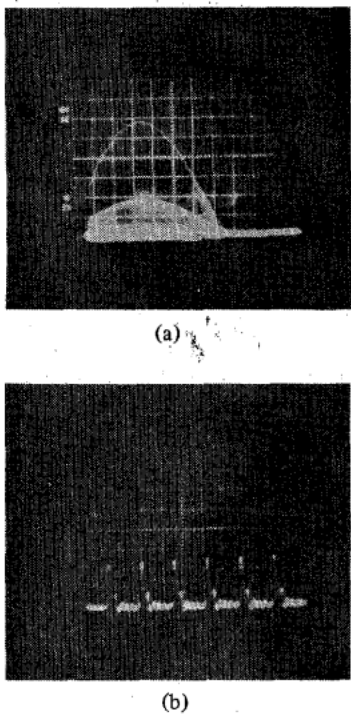


Fig. 4. *Q*-switched and mode-locked output from the Nd:glass laser with OKEM using the transmission function  $C_1$  and  $l = 6$  cm CS<sub>2</sub>. (a) Horizontal 500 ns/div.; vertical 0.50 mJ/div. (b) Horizontal 5 ns/div.; vertical 0.50 mJ/div.

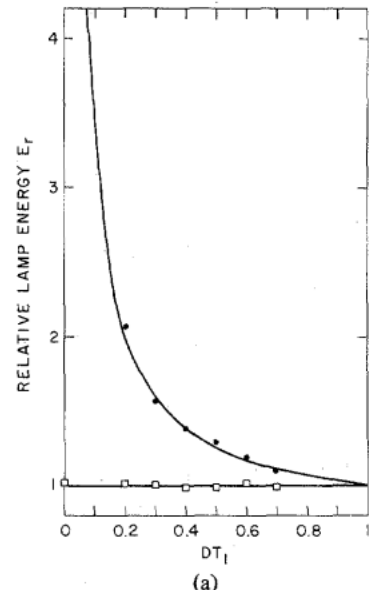
other parameters in the laser constant. These seven transmission functions have equal initial transmissions of  $T_0 = 0.50$  and very similar values for  $J_{IP}$ . The chief difference within these curves are their radically different values of  $DT_I$ . The results of these measurements are shown in Fig. 5(a). The free-running threshold, as expected, remains constant while the threshold for *Q* switching and mode locking is seen to increase asymptotically as  $1/DT_I$ . The data in Fig. 5(a) have been fitted by the equation

$$E_r = 0.738 + \frac{0.263}{DT_I} \quad (27)$$

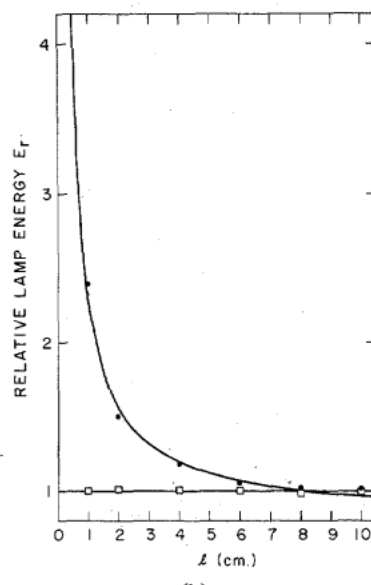
The relative lamp energy  $E_r$  is defined as the lamp energy divided by the measured mean free-running threshold lamp energy. Referring to (20), it is noted that, as with  $DT_I$ , the absolute initial slope varies linearly with the cell length  $l$ . Therefore, to independently verify the behavior described by Fig. 5(a), the lasing threshold was remeasured for the curve  $C_1$  in Table I while varying  $l$  from 1 to 10 cm of CS<sub>2</sub>. The results of these measurements are given in Fig. 5(b) where once again the *Q*-switching and mode-locking threshold is observed to vary asymptotically. The data in this figure have been fitted by the equation

$$E_r = 0.815 + \frac{1.542}{l} \quad (28)$$

Note that mode locking was obtained for a cell length as short as 1 cm of CS<sub>2</sub> using the transmission function  $C_1$ . It is clear from these results that there does not exist any "critical cell length" [5] for mode locking. To verify that (27) was



(a)



(b)

Fig. 5. (a) Threshold energy dependence on the initial slope parameter  $DT_I$ . Free-running threshold (□), mode-locking threshold (●).  $l = 6$  cm CS<sub>2</sub>. (b) Threshold energy dependence of the cell length  $l$ . Free-running threshold (□), mode-locking threshold (●). OKEM transmission curve  $C_1$ .

strictly valid despite the small variation in the value of  $J_{IP}$  for the curves  $C_1$  to  $C_7$ , the *Q*-switching and mode-locking threshold was remeasured as a function of  $DT_I$  using an alternate series of curves which were identical in all respects to the curves  $C_1$  to  $C_7$  but which had consistently larger values for  $J_{IP}$  [these two sets of curves correspond to the two branches of the  $DT_I$  curve given in Fig. 2(a)]. To well within experimental error limits, the results were identical to those shown in Fig. 5(a), thus unambiguously confirming the correctness of (27).

The implication of the results expressed by (27) and (28) is that, in general, the threshold for *Q* switching and mode locking varies as

$$E_{\text{thres}} = A + B[dT_I/dI_0|_{I_0=0}]^{-1} \quad (29)$$

where  $A$  and  $B$  are constants dependent upon the basic param-

eters of the laser. From (20), this threshold dependence may be expressed as

$$E_{\text{thres}} \sim \frac{\lambda}{l \cdot DT_I \cdot \chi_3^{1/2/2}}. \quad (30)$$

Further qualitative confirmation of this dependence was offered by the observation that, for a given transmission function and cell length, the threshold for mode locking with  $C_6H_5NO_2$  was slightly higher than that when using  $CS_2$ .

Passive  $Q$  switching and mode locking of the Nd:glass laser was also obtained using the transmission functions  $C_8$  to  $C_{11}$  of Table I. It was found that the functions  $C_{10}$  and  $C_{11}$  with low values of  $T_0$  generally gave better reproducibility for the laser output than the high initial transmission curves  $C_8$  and  $C_9$ . No anomaly was observed in the increase in the pumping level in changing from transmission curves such as  $C_1$  ( $T_0 = 50$  percent) or  $C_9$  ( $T_0 = 75$  percent) to a curve such as  $C_{11}$  ( $T_0 = 10$  percent). This is noteworthy in view of the behavior described in Fig. 5(a) and the fact that  $DT_I$  for  $C_{11}$  has the relatively small value of 0.18. However some preliminary work on a fluctuation model theory [21]–[24] of the OKEM passively mode-locked laser has led to the finding that the mode-locking threshold should depend not only upon the absolute initial slope as in (29) but rather upon the combined parameter  $dT_I/dI_0|_{I_0=0}/T_0$ . This conclusion, if true, would explain the relative ease in obtaining mode-locking operation for curves such as  $C_{11}$  despite a low  $DT_I$  value since, as Fig. 2(b) indicates, the combined parameter involving  $T_0$  can be large when  $T_0$  is small.

A qualitative explanation may be given of the mode-locking threshold dependence described by Figs. 5(a) and 5(b) in terms of the fluctuation theory of the passively mode-locked laser [4], [21]–[24] and by referring in particular to Fig. 3(b). The critical region [23] corresponding to the selection of a single intense noise fluctuation is roughly that region centered about  $J_0 = 0.01$  in Fig. 3(b) (typically  $I_0 \gtrsim 1 \text{ MW/cm}^2$ ). At this point, the buildup of the noiselike intensity fluctuations changes in nature from a linear process to a nonlinear, intensity-dependent process, since, because of gain depletion and the nonlinearity of the OKEM transmission, the net round-trip laser gain becomes a function of the intensity. Thus the lower intensity fluctuations gradually begin to suffer a reduced net gain (eventually  $<1$ ) since they experience a fixed, nonincreasing OKEM transmission  $T_0$  while the absolute gain in the laser rod is decreasing. The higher intensity fluctuations, however, begin to experience larger transmissions through the OKEM with the result that, even though the gain is depleting, the net gain coefficient for the higher intensity pulses remains positive. The ideal mode-locking situation, corresponding to a pumping level at or very slightly above threshold, is such that there is just sufficient initial gain to allow only the most intense fluctuation to survive and grow to very large peak intensities ( $J_0 \gtrsim 1$ ). At some point, all the other lesser intensity noise fluctuations will induce an OKEM transmission which is insufficient to ensure a net positive round-trip gain coefficient and thus suffer a rapidly increasing attenuation. For a transmission function such as  $C_1$  in Fig. 3(b), this pulse-selection process begins at relatively low intensities. Thus the average intensity of, and hence the net

gain depletion produced by, the ensemble of intensity fluctuations is also limited to relatively small values. Conversely, however, for a transmission function such as  $C_7$  which is essentially flat at low intensities, the average intensity of the fluctuations must grow to a relatively large value before the nonlinear selection of a single fluctuation can occur. This in turn implies the need for a large initial gain in order to be able to amplify all of the large number of noise pulses up to an average of  $J_0 \sim 0.1$ . Thus, from this description, one is led to expect that obtaining  $Q$  switching and mode locking using a transmission curve such as  $C_7$  should require a much higher pumping level than that required when using a transmission function such as  $C_1$ . This expectation is confirmed by the results described in Fig. 5. It is interesting to note that a study of the reproducibility of the saturable absorber mode-locked Nd:glass laser and its dependence on  $T_0$  revealed that the reproducibility was best precisely over that range where the initial slope parameter of the absorber, (26), is a maximum [25].

### C. Pulsewidth and Spectral Measurements

The pulsewidths of the OKEM mode-locked ultrashort pulses were measured using the technique of OKE photography [26]. The experimental arrangement employed was a variation of the transverse-grating focal-plane OKE shutter described in detail elsewhere [8], [13], [27]. Since the pulsewidth measurements were made using the entire mode-locked pulse train, they represent an integrated measurement over the duration of the train. However, it is known that the duration of the individual ultrashort pulses from a passively mode-locked Nd:glass laser increase significantly during the  $Q$  switched pulse envelope [28]. Thus, the measured pulsewidth of  $\approx 20 \text{ ps}$  consistently observed for the OKEM using  $CS_2$  would imply pulsewidths at the beginning of the laser train of a few picoseconds in duration. This is consistent with the analysis offered by Laussade and Yariv [3] which predicts minimum mode-locked pulsewidths  $\approx \tau_0$ , the orientational relaxation time of the liquid used in mode locking ( $\tau_0 \approx 2 \text{ ps}$  in  $CS_2$  [29]). The overall FWHM duration of  $\approx 50 \text{ ps}$  observed for the OKEM using nitrobenzene would imply pulsewidths at the beginning of the pulse train of  $\approx 30\text{--}40 \text{ ps}$  ( $\tau_0$  in  $C_6H_5NO_2$  is  $\approx 32 \text{ ps}$  [30]).

Spectral measurements of the  $1.06\text{-}\mu$  radiation were made using a 0.75-m Czerny-Turner spectrograph (with an instrument dispersion of  $10 \text{ \AA/mm}$ ) and Kodak unsensitized type I-Z plates. The results are shown in Fig. 6 for the laser: 1) free running, 2) mode locked with the Kodak saturable dye 9740, 3) mode locked with the OKEM using a 6-cm cell of  $CS_2$  and the curve  $C_1$  of Table I, and, 4) mode locked using the OKEM with a 10-cm cell of nitrobenzene and the same transmission function. Although not shown, the spectral width for the free-running laser with the OKEM was noticeably broader than the normal free-running laser, Fig. 6(a). The spectra for the mode-locked laser all show an intense narrow line ( $1\text{--}6 \text{ \AA}$  in correctly exposed plates) at the central laser wavelength with a much weaker background extending to higher and lower wavelengths. This background is the result of SPM of the laser radiation. The symmetrical broadening for the saturable dye mode-locked laser is due to the fast electronic Kerr effect in the laser rod itself. The pronounced

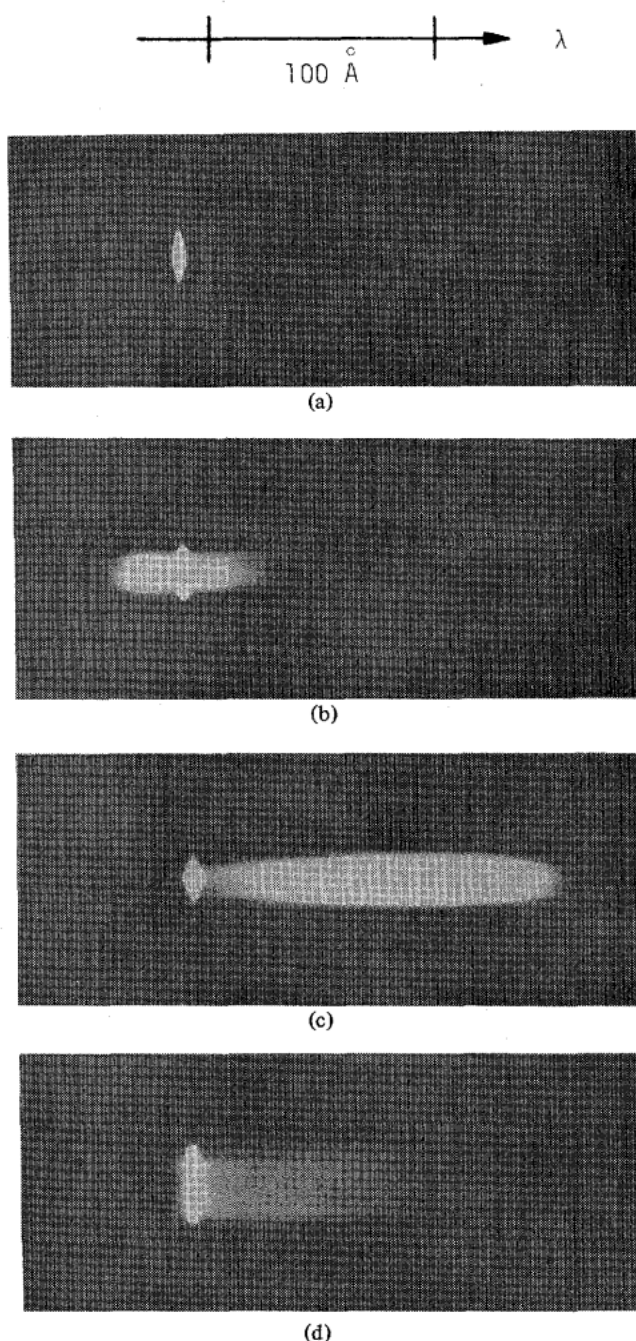


Fig. 6. Spectra from the Nd:glass laser. (a) Free running,  $\lambda_0 = 1.058 \mu$ . (b) Mode locked with Kodak dye 9740. (c) OKEM mode locked using  $CS_2$ . (d) OKEM mode locked using  $C_6H_5NO_2$ .

asymmetry of the spectra in Figs. 6(c) and (d) immediately reveals that, for the OKEM mode-locked laser, the SPM is predominantly due to the presence of the Kerr liquid. An asymmetric SPM spectrum favoring longer wavelengths is a characteristic of media with a large orientational Kerr effect [17], [18]. However, in order to make the SPM readily observable, the spectra in Figs. 6(c) and (d) are grossly overexposed at the central laser wavelength. From correctly exposed plates, the spectral intensity ratio of the central line to the background was estimated to be  $>150$ . Nevertheless, as for the saturable dye mode-locked laser, the presence of SPM in the OKEM mode-locked laser is expected to result in a broadening of the ultrashort pulselwidth along the train.

## V. DISCUSSION

The principal features of the use of the OKEM to passively *Q* switch and mode lock high-power lasers may be summarized as follows.

1) The technique is characteristically simple. For the OKEM employing two  $\lambda/4$  plates, the transmission is described by the simple analytical expression given in (15).

2) The technique is versatile. The laser output properties such as the duration and shape of the *Q*-switched envelope and the peak intensity may be readily changed by simply varying the orientations of the retardation plates and/or varying the length of the cell. As well, the OKEM is able to employ a variety of different OKE media with radically different relaxation times and nonlinear refractive indices.

3) Since the OKEM employs stable liquids such as  $CS_2$  and  $C_6H_5NO_2$ , the transmission characteristics remain constant with time and do not suffer the gradual degradation which affects many saturable dyes. Consequently, mode locking with the OKEM is characterized by excellent long- and short-term stability and pulse reproducibility.

4) The OKEM mode-locking technique is a nonresonant, nonfrequency-selective method. Thus the OKEM may be used with any reasonable high-power laser and should find immediate application for mode locking those lasers for which no fast saturable absorber exists, a principal example being the high-power iodine laser.

As with many saturable dye-switched lasers, the principal undesirable effect in the performance of the OKEM mode-locked laser is the persistence of SPM and its effect on the temporal characteristics of the laser output. One approach to overcoming the problems of SPM is to introduce some passive "saturable transmitter" element into the laser which would limit the radiation buildup to relatively low powers where transform-limited pulses are consistently observed [28]. This may be accomplished by the incorporation of a second OKEM within the resonator which exhibits a saturable transmitterlike behavior [e.g.,  $\theta_1 = \theta_2$  in (15)]. This power limitation approach, however, compromises the basic advantage of the Nd:glass laser to provide very-high-intensity ultrashort pulses. A second approach to overcoming SPM problems lies in designing a spectrally dispersive, high-finesse OKEM which employs suitable multiple-order retarders in a way such that the desired saturable absorberlike transmission exists only over some controlled, narrow spectral range.

## ACKNOWLEDGMENT

The authors wish to thank W. Kennedy, G. Berry, and P. Burtyn for invaluable technical assistance.

## REFERENCES

- [1] P. W. Smith, M. A. Duguay, and E. P. Ippen, "Mode locking of lasers," *Prog. Quantum Electron.*, vol. 3, part 2, 1974.
- [2] R. C. Greenhow and A. J. Schmidt, "Picosecond light pulses," in *Advances in Quantum Electronics*, vol. 2, D. W. Goodwin, Ed. New York: Academic, 1974, pp. 157-286.
- [3] J. Comly, E. Garmire, J. P. Laussade, and A. Yariv, "Observation of mode locking and ultrashort optical pulses induced by anisotropic molecular liquids," *Appl. Phys. Lett.*, vol. 13, pp. 176-178, 1968; J. C. Comly, A. Yariv, and E. M. Garmire, "Stable, chirped, ultrashort pulses in lasers using the optical Kerr effect," *Appl. Phys. Lett.*, vol. 15, pp. 148-150, 1969; J. P. Laussade and A. Yariv, "Mode locking and ultrashort laser pulses by aniso-

tropic molecular liquids," *Appl. Phys. Lett.*, vol. 13, pp. 65-66, 1968; J.-P. Laussade and A. Yariv, "Analysis of mode locking and ultrashort laser pulses with a nonlinear refractive index," *IEEE J. Quantum Electron.*, vol. QE-5, pp. 435-441, Sept. 1969.

[4] W. H. Glenn, "Research investigation of the generation, measurement, and properties of picosecond laser pulses," final rep. AFCRL-72-0275, 1972 (available from National Technical Information Service, Washington, DC).

[5] L. Dahlström, "Passive mode locking and  $Q$ -switching of high power laser by means of the optical Kerr effect," *Opt. Commun.*, vol. 5, pp. 157-162, 1972; —, "Mode locking of high power laser by a combination of intensity and time dependent  $Q$ -switching," *Opt. Commun.*, vol. 7, pp. 89-92, 1973.

[6] A. Gerrard and J. M. Burch, *Introduction to Matrix Methods in Optics*. New York: Wiley, 1975.

[7] P. D. Maker and R. W. Terhune, "Study of optical effects due to an induced polarization third order in the electric field strength," *Phys. Rev.*, vol. 137, pp. A801-A818, 1965; R. Y. Chiao and J. Godine, "Polarization dependence of stimulated Rayleigh-wing scattering and the optical-frequency Kerr effect," *Phys. Rev.*, vol. 185, pp. 430-445, 1969; A. Owyong, R. W. Hellwarth, and N. George, "Intensity-induced changes in optical polarizations in glasses," *Phys. Rev. B*, vol. 5, pp. 628-633, 1972; A. Owyong, "Ellipse rotation studies in laser host materials," *IEEE J. Quantum Electron.*, vol. QE-9, pp. 1064-1069, Nov. 1973.

[8] K. Sala, "Passive mode locking of lasers with the optical Kerr effect modulator," Ph.D dissertation, Dep. of Physics, Univ. of Waterloo, Waterloo, Ont. Canada, Nov. 1976 (available from University Microfilms, Ann Arbor, MI).

[9] A. Owyong, "Absolute determination of the nonlinear susceptibility  $\chi_3$  via two-beam nonlinear interferometry," *Opt. Commun.*, vol. 16, pp. 266-271, 1976.

[10] C. C. Wang, "Nonlinear susceptibility constants and self-focusing of optical beams in liquids," *Phys. Rev.*, vol. 152, pp. 149-156, 1966.

[11] A. Owyong, "The origins of the nonlinear refractive indices of liquids and glasses," Ph.D dissertation, California Inst. of Technol., Pasadena, 1972 (available from University Microfilms, Ann Arbor, MI, 72-22612).

[12] B. Kasprowicz-Kielich and S. Kielich, "A classical treatment of nonlinear processes of molecular relaxation in intense electric fields of high and low frequency," in *Advances in Molecular Relaxation Processes*, vol. 7, pp. 275-305, 1975.

[13] K. Sala, "Picosecond framing photography of second harmonic pulses and laser produced plasmas using an optical Kerr effect shutter," M. Eng. thesis, Carleton Univ., Ottawa, Ont., Canada, 1973.

[14] K. Sala and M. C. Richardson, "Optical Kerr effect induced by ultrashort laser pulses," *Phys. Rev. A*, vol. 12, pp. 1036-1047, 1975.

[15] M. Hercher, "An analysis of saturable absorbers," *Appl. Opt.*, vol. 6, pp. 947-954, 1967.

[16] R. J. Harrach, T. D. MacVicar, G. I. Kachen, and L. L. Steinmetz, "Estimating the peak intensity and energy content of short duration pulses using saturable absorbers," *Opt. Commun.*, vol. 5, pp. 175-178, 1972; G. Girard and M. Michon, "Transmission of a Kodak 9740 dye solution under picosecond pulses," *IEEE J. Quantum Electron.*, vol. QE-9, pp. 979-984, 1973.

[17] R. R. Alfano, L. L. Hope, and S. L. Shapiro, "Electronic mechanism for production of self-phase-modulation," *Phys. Rev. A*, vol. 6, pp. 433-438, 1972; R. A. Fisher and W. K. Bischel, "Numerical studies of the interplay between self-phase-modulation and dispersion for intense plane-wave laser pulses," *J. Appl. Phys.*, vol. 46, pp. 4921-4934, 1975; T. K. Gustafson, J. P. Taran, H. A. Haus, J. R. Lifsitz, and P. L. Kelley, "Self-modulation, self-steepening, and spectral development of light in small-scale trapped filaments," *Phys. Rev.*, vol. 177, pp. 306-313, 1969; V. V. Korobkin, A. A. Malyutin, and A. M. Prokhorov, "Phase self-modulation and self-focusing of neodymium laser radiation with mode locking," *Sov. Phys. -JETP Lett.*, vol. 12, pp. 150-152, 1970; F. DeMartini, C. H. Townes, T. K. Gustafson, and P. L. Kelley, "Self-steepening of light pulses," *Phys. Rev.*, vol. 164, pp. 312-323, 1967.

[18] D. H. Close, C. R. Giuliano, R. W. Hellwarth, L. D. Hess, F. J. McClung, and W. G. Wagner, "82A-The self-focusing of light of different polarizations," *IEEE J. Quantum Electron.*, vol. QE-2, pp. 553-557, Sept. 1966; J. H. Marburger, "Self-focusing: theory," *Progr. Quantum Electron.*, vol. 4, pp. 35-110, 1975.

[19] R. C. Eckardt, C. H. Lee, and J. N. Bradford, "Effect of self-phase modulation on the evolution of picosecond pulses in a Nd:glass laser," *Opt. Electron.*, vol. 6, pp. 67-85, 1974.

[20] This is also a characteristic of the saturable dye mode-locked laser, e.g., R. Wilbrandt and H. Weber, "Fluctuations in mode-locking threshold due to statistics of spontaneous emission," *IEEE J. Quantum Electron.*, vol. QE-11, pp. 186-190, May 1975.

[21] P. G. Kryukov and V. S. Letokhov, "Fluctuation mechanism of ultrashort pulse generation by laser with saturable absorber," *IEEE J. Quantum Electron.*, vol. QE-8, pp. 766-782, Oct. 1972.

[22] J. A. Fleck Jr., "Ultrashort pulse generation by  $Q$ -switched lasers," *Phys. Rev. B*, vol. 1, pp. 84-100, 1970.

[23] W. H. Glenn, "The fluctuation model of a passively mode-locked laser," *IEEE J. Quantum Electron.*, vol. QE-11, pp. 8-17, Jan. 1975.

[24] B. Ya. Zeldovich and T. I. Kuznetsova, "Generation of ultrashort light pulse by means of lasers," *Sov. Phys. Usp.*, vol. 15, pp. 25-44, 1972.

[25] B. Hausherr, E. Mathieu, and H. Weber, "Influence of saturable-absorber transmission and optical pumping on the reproducibility of passive mode locking," *IEEE J. Quantum Electron.*, vol. QE-9, pp. 445-449, Apr. 1973.

[26] M. A. Duguay, "The ultrafast optical Kerr shutter," in *Progress in Optics*, vol. 14, E. Wolf, Ed. New York: North-Holland, 1976, pp. 161-193.

[27] M. C. Richardson and K. Sala, "Picosecond framing photography of a laser produced plasma," *Appl. Phys. Lett.*, vol. 23, pp. 420-422, 1973; K. Sala and M. C. Richardson, "Transverse gating, focal plane, optical Kerr effect photography," to be published.

[28] M. C. Richardson, "Investigation of the characteristics of a mode-locked Nd: glass laser with the aid of a picosecond streak camera," *IEEE J. Quantum Electron.*, vol. QE-9, pp. 768-772, July 1973; D. von der Linde, "Mode locked lasers and ultrashort light pulses," *Appl. Phys.*, vol. 2, pp. 281-286, 1973; D. J. Bradley and W. Sibbett, "Streak camera studies of picosecond pulses from a mode locked Nd: glass laser," *Opt. Commun.*, vol. 9, pp. 17-20, 1973.

[29] S. L. Shapiro and H. P. Broida, "Light scattering from fluctuations in orientations of  $CS_2$  in liquids," *Phys. Rev.*, vol. 154, pp. 129-138, 1967.

[30] P. P. Ho, W. Yu, and R. R. Alfano, "Relaxation of the optical Kerr effect of anisotropic molecules in mixed liquids," *Chem. Phys. Lett.*, vol. 37, pp. 91-96, 1976.